

Cite this: *Green Chem.*, 2012, **14**, 3107

www.rsc.org/greenchem

PAPER

Aqueous phase reforming of glycerol to 1,2-propanediol over Pt-nanoparticles supported on hydrotalcite in the absence of hydrogen†

Chandrashekar Pendem,^a Piyush Gupta,^a Nisha Chaudhary,^a Sarbjit Singh,^a Jagdish Kumar,^a Takehiko Sasaki,^b Arunabha Datta^{‡*} and Rajaram Bal^{**a}

Received 3rd July 2012, Accepted 23rd August 2012

DOI: 10.1039/c2gc36019e

Pt-nanoparticles, in the range of 2–5 nm, supported on hydrotalcite (HT), were used as a catalyst for the selective hydrogenolysis of glycerol to produce 1,2-propanediol by aqueous phase reforming in the absence of any added hydrogen. The catalyst was characterized by XRD, N₂-sorption, pulse chemisorption, TPR, XPS, SEM, TEM, EXAFS. The influence of reaction parameters like reaction time, pressure, *etc.*, were studied in detail. The study reveals that the Pt-nanoparticles are the active sites for the selective conversion of glycerol to 1,2-propanediol. The role of the support also plays an important role in the hydrogenolysis. The hydrogen required for the hydrogenolysis is derived from the reforming of H₂O over the Pt-HT catalyst. The mechanism of the hydrogenolysis reaction is also proposed. A glycerol conversion of 98% with a 1,2-propanediol selectivity of 74% was achieved over 3 wt% Pt supported on HT. The reusability of the catalyst was tested by conducting four runs with the same catalyst and it was found that after four reuses, the conversion and selectivity was almost same.

1 Introduction

The use of renewable feedstock is becoming essential for the sustainable development of society. Much attention has been devoted to applying green catalytic processes to convert bio-renewable feedstocks to commodity chemicals and clean fuels.^{1,2} Glycerol is the by-product in different processes like soap manufacture, fatty acid production, microbial fermentation³ and also during the production of biodiesel by the transesterification of triglycerides. In the production of biodiesel *via* transesterification of triglycerides with methanol, about 1 kg of crude glycerol is formed as a byproduct for every 9 kg of biodiesel. Current disposal of surplus glycerol is used for producing energy by incineration. One concern regarding biodiesel production, is how to handle this by-product. Thus, producing value-added chemicals from glycerol instead of incineration is of great importance for both environmental protection and economic benefit. Research efforts to find new applications for glycerol as a low-cost feedstock for functional derivatives have led to the introduction of a number of selective processes for converting glycerol into commercially valued products. Selective conversion of glycerol is a clean and economically competitive process and represents one

of the most attractive routes, allowing formation of different valuable products, such as 1,2-propanediol (1,2-PDO), 1,3-propanediol (1,3-PDO) or ethylene glycol.^{1,4} Several review papers have been published in recent literature, reporting the utilization of glycerol for chemicals and chemical building blocks.⁵ The glycerol conversion to 1,2-propanediol by catalytic hydrogenolysis has emerged as one of the important processes, as 1,2-propanediol is used as a bulk chemical intermediate for the production of unsaturated polyester resins, as an industrial solvent and anti-freeze, as an approved additive in food, cosmetics and pharmaceutical preparations, and as a lubricant for food machinery.^{4,6–8} 1,2-Propanediol is produced industrially by the hydration of propylene oxide.⁴ There are also reports that nickel, copper chromate, Amberlyst with Ru/C, and CuO/ZnO can be used for the production of 1,2-propanediol from glycerol with the use of expensive external hydrogen. Hydrogenolysis of glycerol to 1,2-propanediol has been reported previously using supported transition metal catalysts such as Ru,^{9–12} Pt,^{12,13} Cu,¹⁴ and Ni,¹⁵ including some bimetallic catalysts consisting of Pt–Ru, Au–Ru, and Ru–Re. In general glycerol reacts with H₂ to form 1,2-propanediol and water *via* consecutive dehydration and hydrogenation reactions.^{16,17} The drawback of these reactions is that expensive H₂ is used. Dumesic and his group reported aqueous phase reforming of glycerol to produce H₂ over Pt supported catalyst, while our idea was to use *in situ* generated H₂ for the hydrogenation reaction.¹⁸ Pt/NaY zeolite,¹³ Pd/Fe₂O₃¹⁹ and an admixture of Pt/Al₂O₃ and Ru/Al₂O₃²⁰ is reported for the conversion of 1,2-propanediol from glycerol in the absence of hydrogen, but in all the cases the TOF (turn over frequency: moles of 1,2-propanediol produced per moles of Pt per unit time) is very low. Herein, we report very high glycerol conversion and 1,2-

^aIndian Institute of Petroleum, Dehra Dun 248 005, India.
E-mail: raja@iip.res.in, adatta@iip.res.in; Fax: +91 135 2660202;
Tel: +91 135 2525797

^bDepartment of Complexity Science and Engineering, University of Tokyo, Japan

† Electronic supplementary information (ESI) available. See DOI: 10.1039/c2gc36019e

‡ Present address: Professor and Head, Centre for Applied Chemistry, Central University of Jharkhand, Ranchi 835205, Jharkhand.

propanediol selectivity with a very high TOF by aqueous phase reforming without the addition of any external hydrogen over 3 wt% Pt supported on hydrotalcite.

2 Experimental

2.1 Materials and preparation of the catalysts

The support hydrotalcite (HT) material was prepared by the reported procedure. $\text{Pt}(\text{NH}_3)_4(\text{NO}_3)_2$ was used as the Pt source and was purchased from Sigma-Aldrich. Glycerol (>99.5%, spectrophotometric grade) was purchased from Sigma-Aldrich and used without further purification. Nitrogen (>99%) was procured from Inox-Air products and used as received.

The Pt supported catalysts were prepared by an incipient wetness impregnation method using $\text{Pt}(\text{NH}_3)_4(\text{NO}_3)_2$ as the Pt precursor. In a typical synthesis procedure 0.185 g $\text{Pt}(\text{NH}_3)_4(\text{NO}_3)_2$ was dissolved in H_2O and 3 g HT was added to it with constant stirring. Then the mixture was dried in a water bath (80 °C) followed by drying in an oven at 110 °C overnight, and further calcined at the required temperature.

2.2 Characterization of the catalyst

The physicochemical characterization of the catalyst and support were characterized by X-ray diffraction (XRD), scanning electron microscopy (SEM), transmission electron microscopy (TEM), X-ray photoelectron spectroscopy (XPS), *etc.* The X-ray diffraction patterns were obtained using $\text{CuK}\alpha$ radiation (40 kV and 40 mA, Advanced Bruker D8 diffractometer). The SEM images were realized by a field emission scanning electron microscope, FEI Quanta 200 F, using a tungsten filament doped with lanthanum hexaboride (LaB6) as an X-ray source, fitted with an ETD detector with a high vacuum mode using secondary electrons and an acceleration tension of 10 or 30 kV. Catalysts were analyzed by spreading them on carbon tape. Energy-dispersive X-ray spectroscopy (EDX) was used in connection with SEM for elemental analysis. The elemental mapping was conducted with the same spectrometer. The surface area of the HT and metal loaded HT were examined by N_2 adsorption-desorption isotherms at 77 K (Belsorbmax, BEL, Japan). TEM images were collected using a JEOL JEM 2100 microscope, and samples were prepared by mounting an ethanol-dispersed sample on a lacey carbon Formvar coated Cu grid. Measurements of the Pt L_{III} -edge extended X-ray absorption fine structure (EXAFS) were carried out at the Photon Factory in the Institute of Materials Structure Science, High Energy Accelerator Research Organization (KEK-IMSS-PF). The measurements were made in transmission mode. Spectra were measured at BL-7C and BL-9C. The electron storage ring was operated at 2.5 GeV and 450 mA. Synchrotron radiation from the storage ring was monochromatized by a Si(111) channel cut crystal. Ionization chambers, which were used as detectors for incident X-ray (I_0) and transmitted X-ray (I), were filled with an Ar (15%)– N_2 mixture gas and Ar (100%) gas, respectively. The EXAFS raw data were analyzed with an UWXAFS analysis package²¹ including background subtraction program AUTOBK²² and a curve fitting program FEFFIT.²³ The amplitude reducing factor, S_0^2 was fixed at 0.95. The backscattering amplitude and phase shift

were calculated theoretically by FEFF 8.4 code.²⁴ ATOMS²⁵ was used to obtain the FEFF input code for crystalline materials. Temperature programmed reduction (TPR) was carried out on a Micromeritics, Auto Chem II 2920 instrument in the temperature range of 50–1000 °C with a heating rate of 10 °C min^{-1} using 10% H_2 –Ar gas as the carrier gas. The H_2 consumed in the TPR study was measured quantitatively by a thermal conductivity detector. Before the TPR study, the catalyst was pre-treated at 350 °C for 2 h under a flow of He. Platinum dispersions were obtained by pulse H_2 -chemisorption. The experiments were carried out in the same setup as H_2 -TPR. Samples were previously reduced under flowing pure H_2 (10 ml min^{-1}) at 500 °C for 2 h, and was then purged in He at 540 °C for 2 h and cooled at 25 °C. The pulse size was 0.5 ml H_2 and the time between pulses was 3 min. A Thermo Scientific K-Alpha X-Ray photoelectron spectrometer was used to study the near surface composition of the dry reforming catalysts before and after the reaction.

2.3 Hydrogenolysis reaction

Hydrogenolysis reactions were conducted in batch mode, in a 160 ml stainless steel autoclave (parr reactor) at various temperatures. The reactor was equipped with a magnetically driven stirrer, a dip tube and an internal water cooling system. The temperature was controlled by a programmable PID controller. Glycerol, catalyst (reduced in H_2 at 480 °C) and water were placed inside the reactor, after which the reactor was closed. Then the system was purged with nitrogen 4 times to remove the air. The whole system was pressurized to 45 bar and the heating was started with a 500 rpm stirring speed. Aliquots (liquid and gas) were withdrawn through the special sample port attached within the reactor. At the end of the reaction, the reactor was cooled down to the room temperature and the pressure was released very slowly. The catalyst particles were separated by filtration and the product was identified using the GC-MS and analyzed by an Agilent 7890 gas chromatograph equipped with a FID (using restek MXT WAX capillary Column 30 m \times 0.25ID), the gaseous product was analyzed by an Agilent 7890 gas chromatograph equipped with a TCD [using packed column molecular sieves 13 \times for H_2 and porapack Q for CO , CO_2 and alkane (C_1 to C_4)].

3 Results and discussion

3.1 Characterization of the catalyst

Typical powder XRD patterns of the hydrotalcite and Pt-loaded hydrotalcite catalyst are shown in Fig. 1. It was observed that the hydrotalcite structure remained intact at 280 °C, and the structure collapsed at 500 °C after calcination in air. We believe that due to the memory effect of hydrotalcite, small instant peaks appear at 12, 25, 35.2 (Fig. 1). The BET surface area estimated by nitrogen adsorption for hydrotalcite (Al_2O_3 – MgO = 80 : 20) was 220 $\text{m}^2 \text{g}^{-1}$ and the surface area reduces to 126 $\text{m}^2 \text{g}^{-1}$ when 3 wt% Pt was loaded.

The morphologies of the Pt-loaded HT catalysts were examined by a scanning electron microscope (SEM). A representative SEM image of the catalyst is shown in Fig. 2A. Pt dispersion of the catalyst was confirmed by EDX (electron dispersive analysis

by X-ray) analysis (ESI, Fig. S1†), and also by H₂ pulse chemisorption techniques. The Pt dispersion results (Pt dispersion, metal surface area, size) carried out by the H₂ chemisorption techniques are shown in Table 1. The high value of dispersion (79.3%) also confirms the homogeneous distribution of Pt over the hydrotalcite support. We have also found that the dispersion is a little bit less (70.9%) when the sample was calcined at 260 °C. The elemental mapping of the catalyst also reveals a homogeneous distribution of Pt on the hydrotalcite support (Fig. 2B). The size of Pt on the support hydrotalcite was analyzed by TEM, and is shown in Fig. 3. From Fig. 3 it can be seen that the average particle size of Pt is about 2–5 nm, which is dispersed throughout the hydrotalcite support. TPR was used to determine the reducible nature of the supported Pt on the hydrotalcite support. Fig. 4 shows the TPR profile of the Pt hydrotalcite calcined at 260 °C and 480 °C. The TPR profile of the Pt-HT sample is composed of two H₂ consumption peaks. The first peak is around 200–300 °C and the second peak is around 440–470 °C. These two peaks are due to two different

types of interacting Pt oxides species, as considered in the literature.^{26,27} The low temperature peak is due to the weak interaction of Pt with the support and the high temperature peak is due to the strong interaction of Pt with the support. We have also measured the Pt 4f_{7/2} XPS spectra to find the oxidation state of the Pt species. Fig. 5 shows the XPS spectra of the catalyst before and after the reaction. The value of 75.1 eV confirms the presence of a Pt²⁺ species before the reaction, and the binding

Table 1 Pt dispersion (H₂ chemisorption) on hydrotalcite (HT)

Catalyst	Pt (%) dispersed	Metal surface area (m ² g ⁻¹)	Active particle size (nm)
Pt-HT (450 °C) ^a	79.3	195.7	1.4
Pt-HT (260 °C) ^b	70.9	175.1	1.6

^a Calcined at 450 °C and reduced at 480 °C. ^b Calcined at 260 °C and reduced at 480 °C at during metal dispersion experiment.

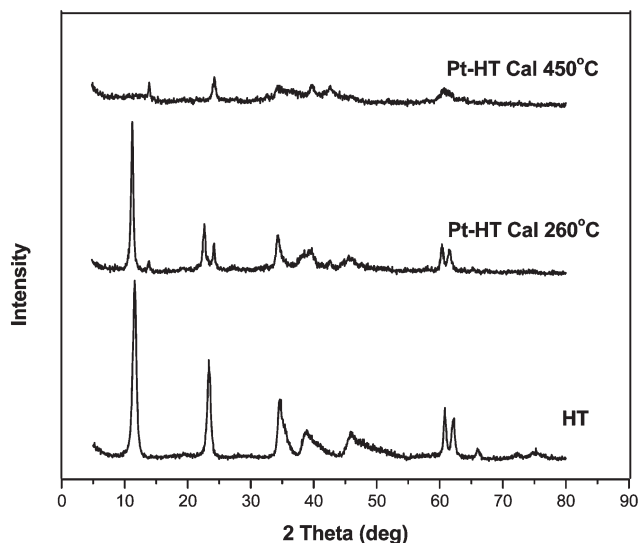


Fig. 1 XRD patterns of prepared hydrotalcite (HT) and Pt-HT calcined at 260 °C and 450 °C.

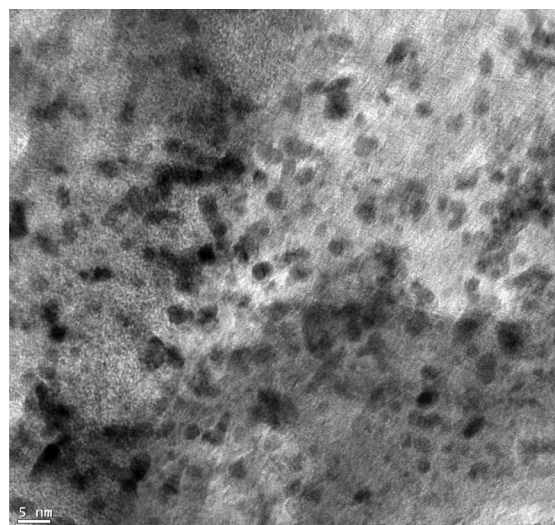


Fig. 3 TEM photograph of Pt-HT sample.

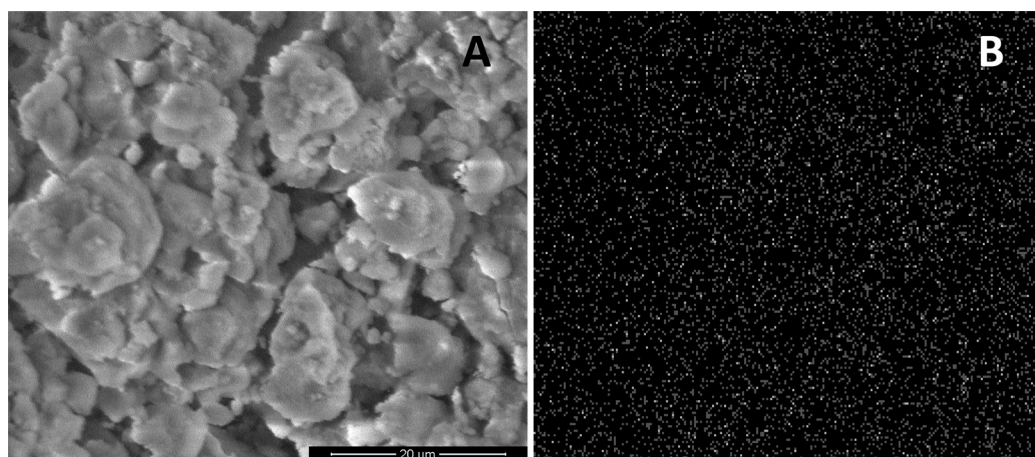


Fig. 2 (A) SEM image of Pt-HT and (B) Pt mapping of Pt-HT sample.

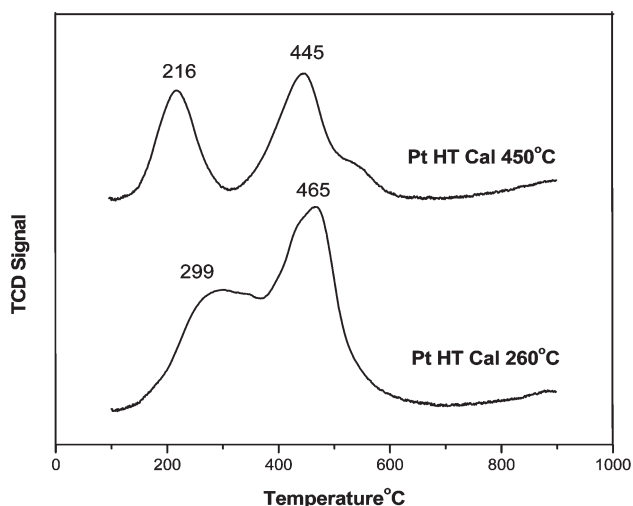


Fig. 4 TPR profile of Pt-HT (Hydrotalcite), calcined at 260 °C and 450 °C.

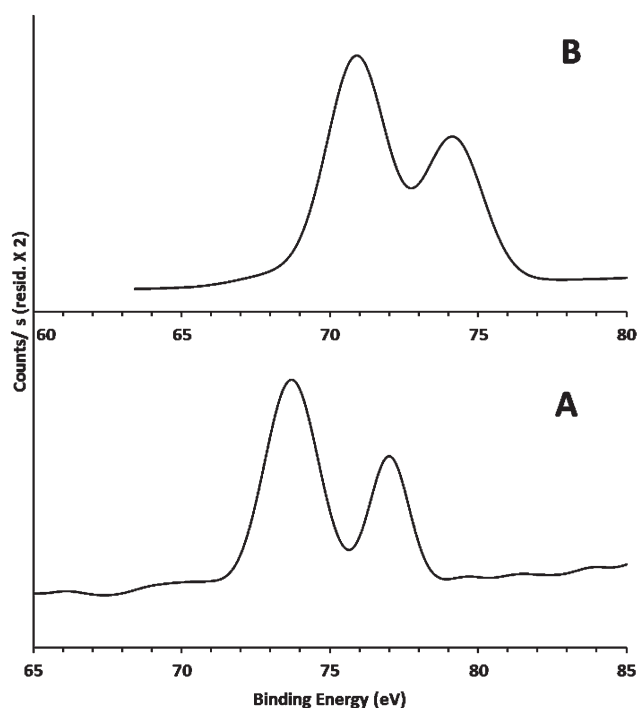


Fig. 5 XPS spectra of Pt (A) before reaction (B) after reaction.

Table 2 EXAFS of the fresh and used Pt-HT catalyst^a

Sample	Shell	Coordination number (CN)	Bond length (nm)	ΔE_0 (eV)
Pt-HT ^b	Pt-O	3.84 ± 0.9	0.2002 ± 0.0012	9.79 ± 1.3
Pt-HT ^c	Pt-Pt	8.49 ± 0.7	0.2772 ± 0.0015	8.76 ± 1.1

^a Fourier-transform spectra ($k = 30\text{--}160 \text{ nm}^{-1}$ and fitted in R space of $R = 0.1\text{--}0.43 \text{ nm}$). ^b Before reaction. ^c After reaction.

energy value of 73.8 eV confirms the presence of metallic Pt after the reaction. EXAFS were also taken for the Pt L_{III}-edge to check the local environment of the Pt species. Table 2 shows the structural parameters of the Pt/HT catalyst determined by curve-fitting of the Pt L_{III}-edge EXAFS data measured at $-258 \text{ }^\circ\text{C}$. EXAFS shows the presence of Pt-O bond at a distance of 0.2002 nm confirms the presence of cationic Pt species with the co-ordination no of 3.84 and the catalyst after the reaction shows the presence of Pt-Pt bond of 0.2772 nm with the co-ordination no of 8.49. Fourier transform Pt L_{III}-edge EXAFS spectra is shown in ESI (Fig. S2[†]).

3.2 Hydrogenolysis reaction

The activities of the different catalysts are shown in Table 3. The products contain both gaseous and liquid products. We have estimated and found that the liquid and gaseous product ratio (C%) was almost 95 : 5. The liquid product contains mainly 1,2-propanediol, ethanol, 2-propanol, 1-propanol, acetol and ethylene glycol (ESI, Table S1[†]). Along with 1,2-propanediol, 2-propanol was obtained as a second major product in the liquid phase. We believe that the formation of 2-propanol from 1,2-propanediol occurs through a dehydration and hydrogenation step, as shown in Scheme 1. The gaseous products contained mainly H₂, and the remaining major gas product was CO₂, along with some light alkanes (ESI, Table S1[†]). It was observed that when only the oxide supports were used, the 1,2-propanediol selectivity was very low. The glycerol conversion was 55.7, 53.0, 45.0, 51.6, 33.7 and the 1,2-propanediol selectivity was 34.8, 19.5, 10.2, 14.2, 8.5, respectively for Pt supported on Al₂O₃, MgO, CeO₂, ZrO₂, SiO₂. Only Pt oxide was also used as the catalyst, but the conversion was only 2% and 1,2-propanediol selectivity was only 5%. As neither Al₂O₃ nor MgO showed good activity or selectivity, it is obvious that hydrotalcite, as a support, definitely has a role in the hydrogenolysis reaction. We also prepared the hydrotalcite with different Al₂O₃ to MgO ratios and found that the activity is less. It has to be noted that the Pt supported on HT forms Pt nanoparticles with sizes of around 2–5 nm. We believe that Pt oxide, of around 2–5 nm in size, is the active species for the reaction, and hydrotalcite with an Al₂O₃ to MgO ratio of 80 : 20 is the optimized ratio to form the 2–5 nm particles. When the Pt was loaded on physically mixed Al₂O₃ and MgO in the ratio of 80 : 20, the Pt nanoparticles were not formed and activity of the catalyst was very low. This also indicates that the HT support favours the formation of highly dispersed 2–5 nm Pt particles. The Pt-supported HT showed a glycerol conversion of 98%, and the liquid products showed a 1,2-propanediol selectivity of 74%. The effect of Pt loading was also investigated. It was found that when the Pt loading was less than 3 wt% the conversion is less, however, the selectivity is higher. On the other hand, when the Pt loading was higher than 3 wt%, the conversion reaches 100% within 1 h but the selectivity of 1,2-propanediol was less (data not shown). So a 3 wt% Pt loading was the optimum loading to get the maximum yield of 1,2-propanediol. The effect of reaction time (ESI, Table S2[†]) shows that the conversion increases but at the same time the selectivity decreases. It was also observed that the glycerol conversion reaches 100% (entry 3, Table 3) when the reaction temperature increases to

Table 3 Activities of the different catalysts^a

Entry	Support	Pt-loading (wt%)	Conv. (mol%)	C _{Sel} (%)	Sel (C%, in liquid products)		TOF (min ⁻¹)
					Sel _{1,2PDO}	Sel _{others}	
1	HT	3	98.4	94.9	70.2	24.7	2.72
2 ^b	HT	3	77.5	95.0	74.4	20.6	2.19
3 ^c	HT	3	100	94.8	48.0	46.8	1.82
4	Al ₂ O ₃	3	55.7	65.8	34.8	31.0	0.73
5	MgO	3	53.0	56.9	19.5	37.4	0.38
6	CeO ₂	3	45.0	45.1	10.2	34.9	0.18
7	ZrO ₂	3	51.6	34.6	14.2	20.4	0.28
8	SiO ₂	3	33.7	56.8	8.5	48.3	0.11
9	PtO	100	2.0	23.9	5.1	18.8	0.00012
10 ^d	Al ₂ O ₃ + MgO	3	51.0	62.2	33.1	29.1	0.64
11 ^e	HT	3	93.1	93.8	67.6	26.2	2.39
Ref. 13	NaY	2.7	85.4	89.4	64.0	25.4	0.24
Ref. 19	Fe ₂ O ₃	Pd = 10	96.0	—	87.0	13.0	0.13
Ref. 20	Al ₂ O ₃	Ru = 5	50.2	—	47.2	52.8	0.35

^a 2 g glycerol in 20 ml water catalyst wt = 0.2 g, reaction time = 3 h and 45 bar N₂, 250 °C. C_{Sel} = carbon selectivity of the total liquid products; TOF = turn over frequency (moles of 1,2-propanediol produced per moles of Pt per unit time). ^b 35 bar N₂, 225 °C. ^c 60 bar N₂, 270 °C. ^d Physically mixed catalyst. ^e Used catalyst (after 4 reuses).

270 °C (ESI, Fig. S3†) and the pressure increases to 60 bar (ESI, Fig. S4†), but the 1,2-propanediol selectivity decreases to 48%. We also carried out the experiment at low temperature and pressure and it was observed that the glycerol conversion decreases to 77.5 (entry 2, Table 3), and the 1,2-propanediol selectivity increases slightly to 74.4%, when the temperature decreases to 225 °C and pressure decreases to 35 bar. So a reaction pressure of 45 bar and a temperature of 250 °C is the optimum reaction conditions for the Pt-supported HT catalyst, in order to obtain the maximum 1,2-propanediol yield. We have also found that when the catalyst to glycerol ratio increases, the conversion increases.

3.3 Proposed reaction pathway and mechanism

Normally, this dehydration reaction occurs at the Brønsted acid sites.^{28,29} It was observed in our reaction, that high amounts of hydroxyacetone (acetol) was formed, and we believe this may be the intermediate for the 1,2-propanediol formation. The proposed mechanism over the Pt-HT catalyst by aqueous phase reforming is shown in Scheme 1. It is assumed that the initial CO₂ formation occurred by catalytic reforming of glycerol and H₂O. This CO₂ aqueous media formed carbonic acid (H₂CO₃) which acts as a Brønsted acid, favouring the dehydration reaction of glycerol to form hydroxyl acetone (acetol). We have also examined the activity of hydroxyacetone instead of glycerol, by carrying out the reaction under similar conditions. It was found that 100% hydroxyacetone conversion was achieved after 3 h, which indicates that hydroxyacetone is the intermediate product. The hydrogenation reaction of acetol to 1,2-propanediol is favoured by the presence of metallic Pt nanoparticles. It has to be noted that the hydrogen required for the hydrogenation reaction is generated *in situ* by the reforming of glycerol. The hydrogenolysis of 1,2-propanediol gives either 1-propanol or 2-propanol under similar reaction conditions.

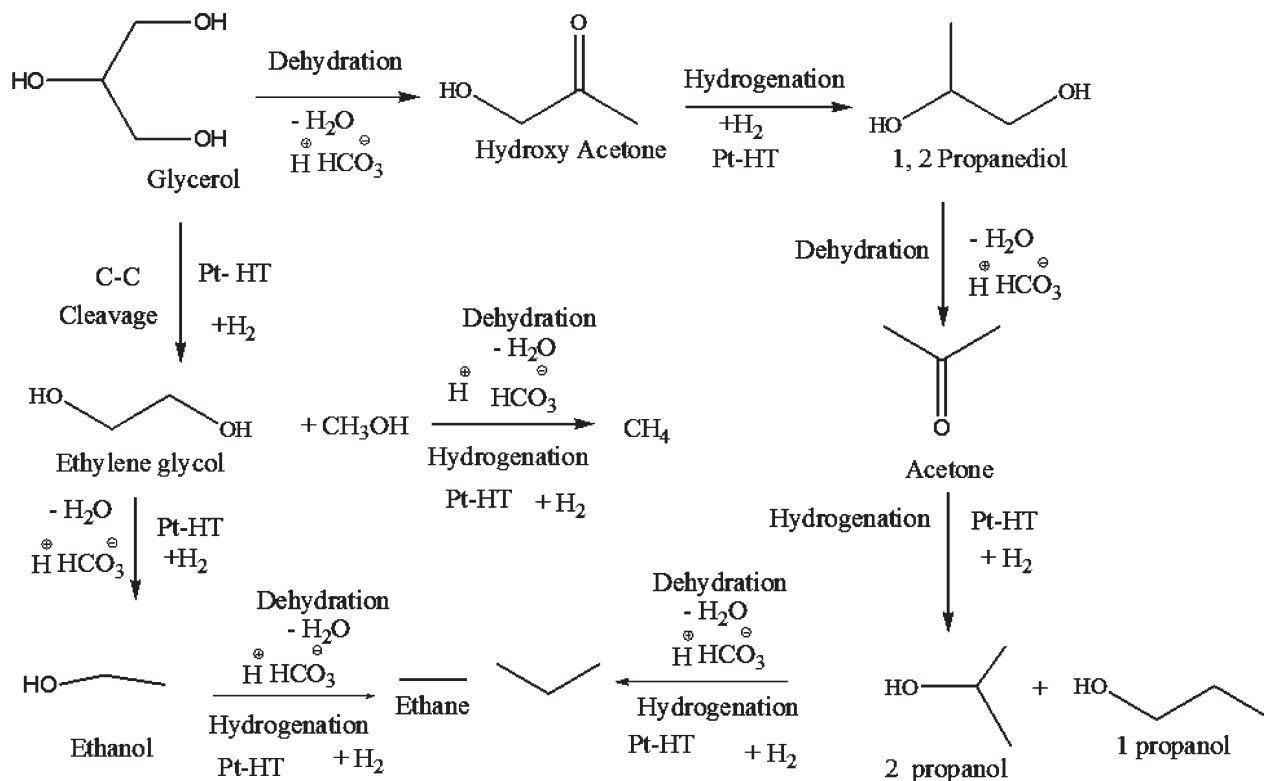
The size of the metallic Pt and also the support, plays a crucial role in the reaction pathway. We have carried out the experiments over Pt supported on individual oxides Al₂O₃ (entry 4, Table 3) and MgO (entry 5, Table 3), but it was observed that the conversion and selectivity were lower. This clearly indicates that Pt nanoparticles of the size 2–5 nm, supported on the HT support, are necessary to obtain the maximum conversion and selectivity.

3.4 Reusability of the catalyst

The reusability of the catalyst was investigated with the same catalyst without any regeneration or activation. The recovered catalyst was washed several times with acetone and dried at 110 °C overnight and was reused directly with fresh glycerol for the hydrogenolysis reaction. The results showed (entry 11, Table 3) that the catalyst remains active after 4 reuses without significant loss of activity. This shows the true heterogeneity of the catalyst. The amount of Pt was estimated by ICP-AES after 4 reuses and it was found that there is no leaching of the Pt.

4 Conclusions

In conclusion, our results show that Pt nanoparticles, of sizes around 2–5 nm, supported on HT are very good catalysts for the conversion of glycerol to 1,2-propanediol with high selectivity and glycerol conversions without the addition of external hydrogen, which is in contrast to other methods reported in the literature for the conversion of glycerol to 1,2-propanediol. Formation of the 2–5 nm particles of Pt is favourable over the support, which is the active species for the selective hydrogenolysis of glycerol to 1,2-propanediol. The 1,2-propanediol selectivity decreases with time. The reusability of the catalyst was tested and it was found that there was no leaching of the catalyst, which supports the true heterogeneity of the catalyst.



Scheme 1 Reaction pathways for aqueous phase reforming of glycerol, for the production of 1,2-propanediol *via* dehydration and hydrogenation steps using the Pt-HT catalyst.

Acknowledgements

The Director, IIP is acknowledged for approving this work. This work was supported by the CSIR in the form of Suprainstitutional Project (SIP 19/4). The XAFS measurements were performed at KEK-IMSS-PF with the approval of the Photon Factory Advisory Committee (project 2010G109).

Notes and references

- 1 C. Zhou, J. N. Beltramini, Y. Fan and G. Q. Lu, *Chem. Soc. Rev.*, 2008, **37**, 527.
- 2 K. Othmer, *Encyclopedia of Chemical Technology*, John Wiley & Sons, Inc., New York, 2001.
- 3 Z. Z. J. Wang, J. Jhugé, H. Fang and B. A. Prior, *Biotechnol. Adv.*, 2001, **19**, 201.
- 4 *Ullman's Encyclopedia of Industrial Chemistry*, Wiley-VCH, Weinheim, 6th edn, 2000.
- 5 M. Pagliaro, R. Ciriminna, H. Kimura, M. Rossi and C. D. Pina, *Angew. Chem., Int. Ed.*, 2007, **46**, 4434.
- 6 J. W. Wabe and D. Eit, *WO 9905085*, 1999.
- 7 T. Fleckenstein, *DE 4302464a1*, 1994.
- 8 P. Gallezot, J. Chaminand, L. Djakovitch, P. Marion, P. Catherine and C. Rosier, *Green Chem.*, 2004, **6**, 359.
- 9 J. Wang, S. Shen, B. Li, H. Lin and Y. Yuan, *Chem. Lett.*, 2009, **38**(6), 572.
- 10 T. Miyazawa, S. Koso, K. Kunimori and K. Tomoshige, *Appl. Catal., A*, 2007, **329**, 30.
- 11 D. G. Lahr and B. H. Shanks, *J. Catal.*, 2005, **232**, 386.
- 12 E. P. Maris and R. J. Davis, *J. Catal.*, 2007, **249**, 328.
- 13 E. D'Hondt, S. Van de Vyver, B. F. Sels and P. A. Jacobs, *Chem. Commun.*, 2008, 6011.
- 14 L. Guo, J. Zhou, J. Mao, X. Guo and S. Zhang, *Appl. Catal., A*, 2009, **367**, 93.
- 15 A. Perosa and P. Tundo, *Ind. Eng. Chem. Res.*, 2005, **44**, 8535.
- 16 C. Montassier, J. C. menez, L. C. Hoang, C. Renaud and J. Barbier, *J. Mol. Catal.*, 1991, **70**, 99.
- 17 R. Connor, K. Folkers and H. Adkins, *J. Am. Chem. Soc.*, 1932, **54**, 1138.
- 18 R. D. Cortright, R. R. Davda and J. A. Dumesic, *Nature*, 2002, **418**, 964.

-
- 19 M. G. Musolino, L. A. Scarpino, F. Mauriello and R. Pietropaolo, *Green Chem.*, 2009, **11**, 1511.
- 20 D. Roy, B. Subramanian and R. V. Chaudhari, *Catal. Today*, 2010, **156**, 31.
- 21 E. A. Stern, M. Newville, B. Ravel, Y. Yacoby and D. Haskel, *Phys. B*, 1995, **208–209**, 117.
- 22 M. Newville, P. Livins, Y. Yacoby, E. A. Stern and J. J. Rehr, *Phys. Rev. B*, 1995, **47**, 14126.
- 23 A. L. Ankudinov, B. Ravel, J. J. Rehr and S. D. Conradson, *Phys. Rev. B*, 1998, **58**, 7565.
- 24 A. L. Ankudinov, A. I. Nesvizhskii and J. J. Rehr, *Phys. Rev. B*, 2003, **67**, 115120.
- 25 B. Ravel, *J. Synchrotron Radiat.*, 2001, **8**, 314.
- 26 E. Merlin, P. Beccat, J. C. Bertolini, P. Delichere, N. Zanier and B. Didillon, *J. Catal.*, 1996, **159**, 178.
- 27 H. Liezke, G. Lietz, H. Spindler and J. Volter, *J. Catal.*, 1983, **81**, 8.
- 28 C. W. Chiu, M. A. Dasari and G. J. Suppes, *Am. Inst. Chem. Eng.*, 2006, **52**, 3543.
- 29 G. J. Suppes, M. A. Dasari, P. Kiatsimkul and W. R. Sutterlin, *Appl. Catal., A*, 2005, **281**, 225.